75th International Astronautical Congress (IAC), Milan, Italy, 14-18 October 2024.

IAC-24-A6-IP-99-x86687

Fair Shared Collision Avoidance Manoeuvre for Active vs Active Conjunctions

J. Rubio[ab]*, F. Biondi[ac], D. Escobar[a], P. Di Lizia[c]

[a] *GMV Aerospace and Defence, Calle Isaac Newton 11, Tres Cantos, 28670, Spain,* jorge.rubio.anton@gmv.com, fbiondi@gmv.com, descobar@gmv.com

[b] *Universidad Carlos III de Madrid, Avenida Universidad 30, Leganés, 28911, Spain,* jorge.r.anton@alumnos.uc3m.es

[c] *Politecnico di Milano, Via G. La Masa 34, Milan 20156, Milan, Italy,* fausto.biondi@mail.polimi.it, pierluigi.dilizia@polimi.it

* Corresponding Author

Abstract

The New Space era has led to the proliferation of small satellites and the deployment of mega-constellations, resulting in an increase in high-risk close approaches between manoeuvrable satellites. This scenario necessitates the development of innovative solutions to mitigate collision risk and to promote sustainable and responsible satellite design and operations. In the context of Space Traffic Management, ongoing efforts are focused on developing procedures and algorithms to enhance the quality and effectiveness of collision avoidance manoeuvres (CAMs). Currently, there is a trend towards establishing rules of the road to determine right-of-way in high-risk collision scenarios between active satellites, thereby specifying which satellite should execute the manoeuvre. This work investigates an alternative approach to managing high-risk active versus active conjunctions, namely the execution of shared CAMs. In this strategy, both satellites undertake a coordinated CAM, with the cost of the mitigation action being distributed between them. For this approach to succeed, it must ensure fairness for all parties involved. Additionally, to garner international support, it must also promote the sustainable and responsible use of space. To that end, this work introduces the concept of fairness in the optimisation of shared CAMs by distributing the manoeuvring effort based on each satellite's contribution to the collision risk. Parameters such as object size and orbital uncertainty are incorporated into the definition of a fairness factor, which relates the control effort of both satellites and ensures an equitable distribution. The fairness factor aims to favour satellites with more accurate orbital information (i.e. smaller covariance at the time of closest approach, TCA), which may result from factors such as data sharing, individual sensor observations, or the use of materials and satellite sizes that are more easily detected by SST sensors. Simultaneously, it also considers each satellite's contribution to the combined hard-body radius, which affects the collision probability. The problem is formulated as an optimal control problem, where the objective is to minimise the total manoeuvring effort subject to an acceptable risk level threshold. Finally, a real conjunction between two manoeuvrable satellites is analysed to demonstrate the advantages of this collision avoidance strategy.

Keywords: *space traffic management, collision avoidance, shared collision avoidance manoeuvre*.

Nomenclature

$\boldsymbol{A}$	=	auxiliary matrix used to generalise the NLP problem to accommodate different types of constraints; see Eqs. (10)-(12)
$\widetilde{\boldsymbol{A}}_{ij}$	=	auxiliary matrix used to simplify the resolution of the NLP problem for the propellant-optimal shared CAM; see Eq. (17)
$\tilde{a}_{ij}$	=	central diagonal element of the matrix $\widetilde{\boldsymbol{A}}_{ij}$
$\boldsymbol{A}_\eta$	=	auxiliary matrix used to simplify the resolution of the NLP problem for the fair shared CAM; see Eq. (34)
a_η	=	second element of the main diagonal of $\boldsymbol{A}_\eta$
$\alpha_{c,i}$	=	flight path angle of S_i at the TCA
$\boldsymbol{b}_i$	=	auxiliary vector used to simplify the resolution of the NLP problem for the propellant-optimal shared CAM; see Eq. (22)
b_i	=	central component of the vector $\boldsymbol{b}_i$
$\boldsymbol{b}_\eta$	=	auxiliary vector used to simplify the resolution of the NLP problem for the fair shared CAM; see Eq. (35)
b_η	=	central component of the vector $\boldsymbol{b}_\eta$
β_i	=	angle that relates $\langle x,y,z\rangle_i$ to $\langle \xi,\eta,\zeta\rangle$ when S_i manoeuvres

$\boldsymbol{C}_i$ = position covariance matrix of S_i
$\boldsymbol{C}_{\xi\zeta}$ = relative position covariance submatrix in (ξ, ζ) B-plane axes; see Eq. (14)
$d_{B,2D}$ = B-plane miss distance
d = total miss distance
$\boldsymbol{D}_i$ = matrix used to compute $\boldsymbol{M}_i$ that accounts for the orbital dynamics; see Eq. (3)
δ = auxiliary scalar used to generalise the NLP problem to accommodate different types of constraints; see Eqs. (10)-(12)
$\Delta\boldsymbol{r}_f$ = final relative position between the objects after the execution of the shared CAM; see Eq. (6)
δt = time shift produced by the manoeuvre of S_i
δr_i = in-plane radial shift produced by the manoeuvre of S_i
δw_i = out-of-plane shift produced by the manoeuvre of S_i
$\Delta\bar{t}_i$ = non-dimensional manoeuvre lead time of S_i
$\Delta\theta_i$ = angular step used to define the manoeuvre true anomaly search space
$\Delta\boldsymbol{v}_i$ = manoeuvre impulse vector of S_i
Δv_i = manoeuvre impulse magnitude of S_i
$\Delta\bar{v}_i$ = non-dimensional manoeuvre impulse magnitude of S_i
$\Delta v_{i,max}$ = maximum manoeuvre impulse magnitude of S_i
$e_{0,i}$ = unperturbed orbit eccentricity of S_i
$\langle\xi, \eta, \zeta\rangle$ = B-plane reference system
η = general fairness factor
η_s = fairness factor based on the satellites' HBRs; see Eq. (26)
η_u = fairness factor based on the satellites' orbital uncertainty; see Eq. (26)
$f(\boldsymbol{x})$ = objective function of the NLP problem
$g(\boldsymbol{x})$ = equality constraint of the NLP problem
HBR_i = hard-body radius of S_i
γ_0 = auxiliary scalar used to simplify the resolution of the NLP problem; see Eqs. (17) and (32)
i = satellite index, with 1 denoting the primary and 2 the secondary
$\boldsymbol{I}$ = identity matrix
J = global cost function; see Eq. (39)
J_{min} = minimum value of the global cost function
k = iterative index to define the manoeuvre true anomaly search space
$\boldsymbol{K}_i$ = matrix used to compute $\boldsymbol{M}_i$ that accounts for the orbital kinematics; see Eq. (4)
λ = Lagrange multiplier
$\mathcal{L}(\boldsymbol{x}, \lambda)$ = Lagrangian function of the method of Lagrange multipliers; see Eq. (19)
$\boldsymbol{M}_\eta$ = auxiliary matrix used to simplify the resolution of the NLP problem for the fair shared CAM; see Eq (33)
$\boldsymbol{M}_i$ = state transition matrix of S_i; see Eq. (2)
μ = Earth's standard gravitational parameter
N = total number of points of the manoeuvre true anomaly search space
ϕ_i = angle describing the relationship between the orbital velocity vectors of the two satellites at the TCA when S_i manoeuvres
ψ_i = angle describing the relationship between the orbital velocity vectors of the two satellites at the TCA when S_i manoeuvres
$\boldsymbol{Q}$ = matrix used to compute $\boldsymbol{A}$ when $d_{B,2D}$ is selected as collision risk metric; see Eq. (13)
$\boldsymbol{Q}^*$ = matrix used to compute $\boldsymbol{A}$ when SMD is selected as collision risk metric; see Eq. (13)
$\boldsymbol{r}_0$ = predicted miss distance before the execution of the CAM
R_c = combined hard-body radius
$\boldsymbol{r}_i$ = orbital position vector of S_i after the execution of the shared CAM
$\boldsymbol{R}_i$ = matrix used to compute $\boldsymbol{M}_i$ that accounts for the orbital kinematics; see Eq. (5)
$\langle r, \theta, h\rangle_i$ = local RTN reference frame of S_i
S_i = satellite i
SMD = squared Mahalanobis distance
t_{ref} = reference orbital velocity used to compute $\Delta\bar{t}_i$
$\theta_{c,i}$ = orbital true anomaly of S_i at the predicted TCA
$\theta_{m,i}$ = orbital true anomaly at which S_i executes the manoeuvre
$\theta_{m,i}^k$ = k-th element of the manoeuvre true anomaly search space; see Eq. (38)
$\boldsymbol{v}_i$ = unperturbed orbital velocity vector of S_i
v_i = unperturbed orbital velocity magnitude of S_i
v_{ref} = reference orbital velocity used to compute $\Delta\bar{v}_i$
$\boldsymbol{x}$ = optimisation variable of the NLP problem
$\langle x, y, z\rangle_i$ = auxiliary inertial reference frame at the S_1-S_2 impact point when S_i manoeuvres
w_1, w_2 = weighting factors associated with the CAM optimisation strategy

Acronyms/Abbreviations

CA	Collision Avoidance
CAM	Collision Avoidance Manoeuvre
CSS	Chinese Space Station
ESA	European Space Agency
HBR	Hard-Body Radius
IADC	Inter-Agency Space Debris Coordination Committee
ISRO	Indian Space Research Organisation
LEO	Low Earth Orbit
NASA	National Aeronautics and Space Administration
NLP	Nonlinear Programming
O/O	Owner/Operator
RotR	Rules of the Road
RTN	Radial-Transverse-Normal
SST	Space Surveillance and Tracking
STM	Space Traffic Management
TCA	Time of Closest Approach
UN	United Nations

1. Introduction

Since the dawn of the space age on October 4, 1957, with the launch of Sputnik-1, the world's first artificial satellite, the number of human-made objects orbiting the Earth has steadily increased due to strategic military interests, the advance of scientific research, and the emergence of commercial opportunities. In recent years, however, there has been an exponential rise in the number of satellites launched into space with the advent of the New Space era, which has significantly expanded access to outer space. This paradigm shift in space utilisation is characterised by the growing involvement of private companies, facilitated by technological advancements such as satellite miniaturisation and reusable rocket technology, which have markedly reduced manufacturing and launch costs. Concurrently, renewed geopolitical competition, involving both traditional and emerging space-faring nations, has also intensified the congestion of the space environment.

As of August 2024, approximately 35,940 space objects are regularly monitored by space surveillance networks, of which around 10,100 are operational satellites [1]. The remainder comprises non-functional satellites and other forms of space debris, including spent rocket stages and fragments resulting from accidental explosions, material degradation, deliberate detonations, and in-orbit collisions. In this context, the issue of in-orbit collisions extends beyond the immediate damage to satellites caused by impacts with space debris or other satellites. Such collisions generate debris fragments that can lead to further collisions among these fragments and other satellites, potentially triggering a self-sustained growth of the space debris population, a phenomenon known as the "Kessler Syndrome" [2]. As a result, some orbital regions may become unusable, with potentially catastrophic social and economic consequences due to the dependence of communication, commercial, and security systems on satellite-based information.

Fig. 1 illustrates the congestion in near-Earth orbital regions, specifically highlighting the number of objects in the LEO IADC protected region, which spans altitudes below 2000 km. This orbital region is of critical importance for communication and Earth observation missions and should be cleared from permanent or (quasi-) periodic presence of non-functional artificial objects [3]. As it can be observed, the majority of operational objects are concentrated within a few narrow bands around 500 km altitude. These satellites predominantly belong to the Starlink mega-constellation, which provides global broadband internet coverage.

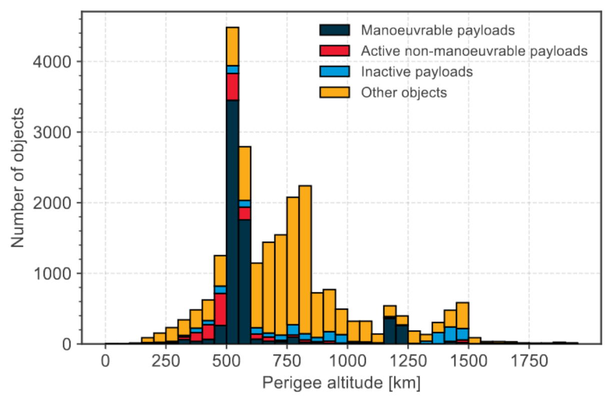

Fig. 1. Number of manoeuvrable and active LEO objects [3]

The number of satellite constellations is expected to rise in the coming years, with many companies planning to deploy mega-constellations —defined as those comprising more than 500 satellites— primarily within LEO. These extensive clusters will contribute substantially to the projected growth of the space population. As of July 2024, SpaceX has in orbit over 6,200 satellites as part of its Starlink mega-constellation [4][5], with approval from the U.S. Federal Communications Commission to launch up to 12,000 satellites [6]. Eutelsat OneWeb's satellite communications network currently includes more than 630 satellites in LEO [7]. Other actors are also entering the race to provide low-latency, high-speed broadband internet access. For example, China aims to develop GuoWang, a mega-constellation of 12,992 satellites [8], and Amazon plans to deploy Project Kuiper, which will consist of 3,232 satellites [9], both also situated in LEO.

The rapid proliferation of artificial objects in Earth's orbit, significantly accelerated by the deployment of mega-constellations, emphasises the urgent need for a comprehensive Space Traffic Management (STM) regulatory framework to ensure effective coordination among satellite Owners/Operators (O/Os) and other stakeholders, and to proactively implement collision risk mitigation strategies. However, currently, there is no universally binding international treaty or regulation that mandates compliance for all entities involved in space activities. Meanwhile, high-risk conjunctions between orbiting satellites are becoming increasingly frequent. Particularly concerning are the high-risk close approaches involving active, manoeuvrable satellites, which were previously rare but now present a substantial challenge to the safety and effective management of space operations.

Noteworthy examples of close encounters between active manoeuvrable satellites include the incident involving ESA's Aeolus and SpaceX's Starlink-44 satellites. In this case, early communication with SpaceX allowed ESA to implement a mitigation strategy after confirming that the Starlink satellite would maintain its nominal trajectory without executing any risk mitigation action [10]. Another significant case involved ISRO's Chandrayaan-2 and NASA's Lunar Reconnaissance Orbiter, where both agencies recognised the need for a CAM, ultimately leading to the joint decision for Chandrayaan-2 to perform the necessary risk mitigation action [11]. Additionally, in a 2021 note verbale to the UN, China reported two close encounters between the Chinese Space Station (CSS) and SpaceX's Starlink-1095 and Starlink-2305 satellites. These encounters required CAMs by the CSS to ensure the safety of its astronauts. In response, the United States, on behalf of SpaceX, stated that the United States Space Command had assessed the collision risk as below the emergency threshold and was unaware of any contact or attempted contact from China regarding the incidents [12].

These events demonstrate the urgent need to standardise CA procedures for all stakeholders involved in space activities. The current approach, where O/Os negotiate ad-hoc risk mitigation actions in coordination with CA service providers is increasingly unsustainable due to the exponential growth in space traffic. Moreover, the communication protocol is not standardised, and the absence of legal obligations often results in the O/O most concerned about the risk being the one to execute the CAM. To better manage the increasing volume of space traffic and mitigate the risk of in-orbit collisions between operational, manoeuvrable satellites, various strategies and decision-making processes have been proposed in recent years. The two most extensively studied strategies are rule-based and negotiation-based approaches.

On the one hand, rules of the road (RotR) are a set of regulations and procedures that determine the right-of-way for satellites, dictating which satellite must execute a CAM based on predefined criteria and parameters that are evaluated and compared. This approach minimises the need for communication between parties involved in resolving a conjunction event, thereby enabling full automation and seamless integration into a STM framework. The concept of space RotR has been under development since the early 2000s, initially drawing on principles from air law [13]. Subsequent research has proposed specific prioritisation criteria that focus on satellite manoeuvrability [14]-[16], the value and ownership of space assets [17] or a combination of these considerations, along with additional factors such as the satellites' orbits, physical characteristics, technical capabilities, and mission types [18][19].

On the other hand, negotiation-based strategies focus on reaching a consensus among the O/Os involved in a conjunction event regarding the mitigation actions required to reduce collision risk. Several models have been proposed, including an auction-based system in which O/Os bid to take responsibility for resolving the conjunction. In this system, the O/O proposing the lowest cost for the CAM receives that amount from the other O/O [14][15]. Another proposed approach is the double offer strategy, where O/Os express their preference for either executing a CAM or not by using virtual currency. This virtual currency is exchanged based on their offers and is employed to reward cooperative behaviour and penalise irresponsible actions [20].

Another interesting cooperative strategy for mitigating collision risk between active manoeuvrable satellites is the shared CAM, where O/Os agree to distribute the manoeuvring effort between the two satellites in collision course. Despite its potential, this strategy has received limited attention in the literature. Michel et al. [18] suggest it as a potential decision-making process for conjunction resolution. Nag et al. [15] discuss the possibility of splitting the manoeuvre costs equally, whether in terms of propellant consumption, mission disruption, or other mutually agreed-upon parameters. The study emphasises the simplicity of such agreements, as they do not require additional compensation. However, it also notes challenges, such as quantifying mission disruption and the need for extensive communication to coordinate manoeuvres. From a technical perspective, Venigalla et al. [21] examined coordinated shared CAMs by posing the CA problem as a multi-objective optimisation problem with a specified miss distance constraint, and explored the Pareto-optimal trade-offs in propellant consumption for each satellite.

The present work focuses on further investigating the shared CAM approach for resolving conjunction events between active manoeuvrable satellites. This strategy shows potential for garnering international support, especially through the fair shared CAM concept introduced in this study, which optimises manoeuvres for propellant efficiency while fairly distributing the manoeuvring effort based on each satellite's contribution to the collision risk. This shared CAM approach is designed to be fair, transparent, effective, and objective, and therefore has the potential to become a cornerstone in the development of international STM regulations and in ensuring the adherence of satellite O/Os to them.

This work presents a novel methodology for designing and optimising shared CAMs based on a Nonlinear Programming (NLP) problem with probabilistic or geometric constraints. Two formulations are proposed: one that focuses exclusively on propellant efficiency by optimising the manoeuvres of each satellite independently, and another that incorporates a fair distribution of manoeuvring effort based on each satellite's contribution to the collision risk. To demonstrate the effectiveness of the fair shared CAM, a real high-risk conjunction event is analysed. The performance of the fair shared CAM is compared with that of the propellant-optimal shared CAM and the individual CAMs, which would be required if only one satellite were to perform the manoeuvre. The results provide insights into the optimality of the fair shared CAM with respect to propellant consumption, as well as its superior flexibility in efficiently mitigating collision risk in operational scenarios.

2. Methodology

This section presents the methodology developed for the design and optimisation of shared CAMs. Firstly, the analytical formulation for designing an impulsive manoeuvre is outlined. Subsequently, the manoeuvre impulses of the two satellites in collision course are optimised by posing the problem as a Nonlinear Programming (NLP) problem, with fixed manoeuvres execution times. The optimisation focuses on propellant efficiency while ensuring compliance with a predefined collision risk threshold. As anticipated in Section 1, two formulations of the shared CAM are analysed: the first involves each satellite independently contributing to the shared CAM, with the objective of minimising the overall manoeuvring effort, while the second introduces a fairness factor to ensure a fair distribution of the manoeuvring effort based on each satellite's contribution to the collision risk. Finally, the general optimisation problem is presented, incorporating the timing of manoeuvre execution as an additional optimisation variable and considering various design strategies.

2.1. Shared CAM effect on relative dynamics

To begin with, a formulation must be developed to assess the impact of the shared CAM on the collision risk metrics of a conjunction event between two satellites. The analytical formulation proposed by Bombardelli [22] for a CAM executed by a single satellite has been selected as the foundation for designing and optimising shared CAMs. Before providing a detailed explanation of the specifics of shared CAMs, it is worthwhile to briefly describe the main characteristics of Bombardelli's method and how it has been adapted to the shared CAM scenario, where both active satellites in a potential collision execute a CAM, rather than just one.

Bombardelli's method assumes elliptical Keplerian orbits and utilises generalised Peláez orbital elements to derive an analytical expression for computing the relative dynamics of two objects in collision course after a CAM is executed by the primary object S_1, i.e. a protected operational satellite capable of manoeuvring. In this approach, the manoeuvre impulse $\Delta\boldsymbol{v}_1$ is first mapped to time, in-plane radial and out-of-plane shifts $(\delta t, \delta r, \delta w)_1$. These shifts are then converted into a change in the pre-manoeuvre position vector at the predicted TCA, expressed within an auxiliary inertial reference frame $\langle x, y, z\rangle_1$ centred at the S_1-S_2 impact point. The resulting displacement vector is subsequently rotated into the collision B-plane reference system $\langle \xi, \eta, \zeta\rangle$, which is defined under the assumption of a short-term encounter. This method ultimately provides a closed-form analytical solution that maps the manoeuvre impulse $\Delta\boldsymbol{v}_1 = [\Delta v_r, \Delta v_\theta, \Delta v_h]_1^T$ expressed in the local Radial-Transverse-Normal (RTN) reference frame $\langle r, \theta, h\rangle_1$, to a displacement $\Delta\boldsymbol{r}_1 = [\Delta\xi, \Delta\eta, \Delta\zeta]_1^T$ in the B-plane axes.

Previously, the subscript 1 was used to denote quantities and reference frames associated with the scenario where only one satellite, S_1, executes the CAM. Hereafter, a general subscript $i = 1, 2$ will be used to indicate that in the shared CAM scenario, both objects involved in the conjunction may execute a manoeuvre. Therefore, the analytical expression that maps the manoeuvre impulse of satellite S_i into a displacement in the B-plane at the TCA is given by:

$$\Delta\boldsymbol{r}_i = \boldsymbol{R}_i\boldsymbol{K}_i\boldsymbol{D}_i\Delta\boldsymbol{v}_i = \boldsymbol{M}_i\Delta\boldsymbol{v}_i \tag{1}$$

where the state transition matrix is:

$$\boldsymbol{M}_i = \boldsymbol{R}_i\boldsymbol{K}_i\boldsymbol{D}_i \tag{2}$$

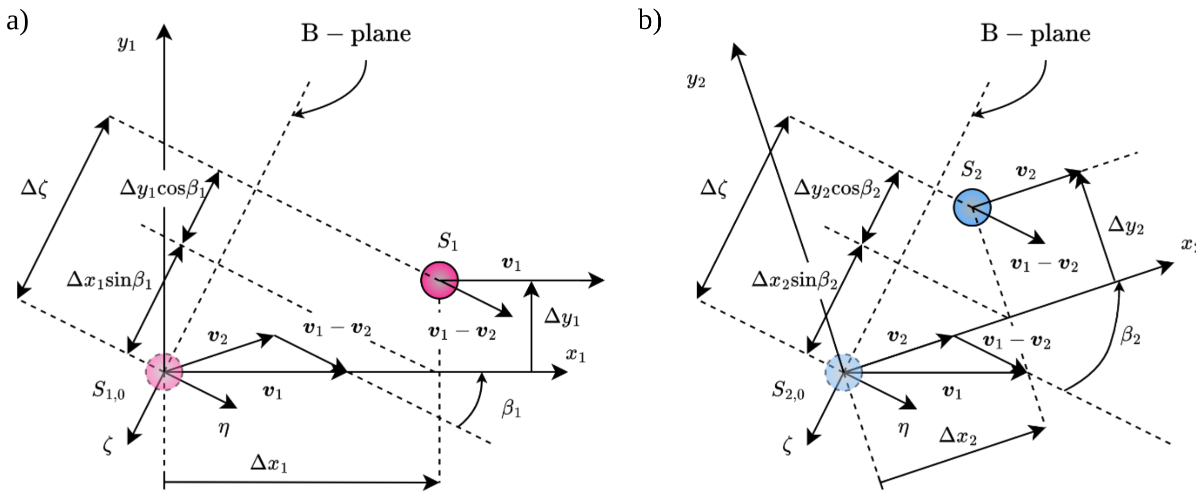

Fig. 2. Auxiliary inertial reference frames and β_i definition for (a) S_1, and (b) S_2

The definition of the parameters within $\boldsymbol{R}_i$, $\boldsymbol{K}_i$ and $\boldsymbol{D}_i$, —such as those related to the equations governing the perturbed orbital motion— need to be adapted to modify Bombardelli's method for the scenario where both objects execute a manoeuvre rather than just one.

The matrix $\boldsymbol{D}_i$ accounts for the collision avoidance dynamics by performing the mapping $\Delta\boldsymbol{v}_i \rightarrow (\delta t, \delta r, \delta w)_i$, under the assumption that the manoeuvre impulse is small compared to the velocity of satellite S_i, and is defined as:

$$\boldsymbol{D}_i = \sqrt{\frac{R_c^3}{\mu}} \begin{bmatrix} d_{tr,i} & d_{t\theta,i} & 0 \\ d_{rr,i} & d_{r\theta,i} & 0 \\ 0 & 0 & d_{wh,i} \end{bmatrix} \quad (3)$$

where the terms $d_{tr,i}$, $d_{t\theta,i}$, $d_{rr,i}$, $d_{r\theta,i}$ and $d_{wh,i}$ are non-dimensional functions of the unperturbed orbit eccentricity $e_{0,i}$ of the manoeuvring satellite S_i, the orbital true anomaly at which its CAM is executed $\theta_{m,i}$, and its orbital true anomaly at the predicted TCA $\theta_{c,i}$.

Matrices $\boldsymbol{K}_i$ and $\boldsymbol{R}_i$ account for the kinematics, specifically the transformations $(\delta t, \delta r, \delta w)_i \rightarrow (\delta x, \delta y, \delta z)_i \rightarrow \Delta\boldsymbol{r}_i$, and are given by:

$$\boldsymbol{K}_i = \begin{bmatrix} -v_i\sqrt{\frac{R_c}{\mu}} & \sin\alpha_{c,i}\sin\theta_{c,i} & 0 \\ 0 & -\frac{\cos\alpha_{c,i}\sin\phi_i\cos\psi_i}{\sqrt{1-\cos^2\psi_i\cos^2\phi_i}} & \frac{\sin\psi_i}{\sqrt{1-\cos^2\psi_i\cos^2\phi_i}} \\ 0 & \frac{\cos\alpha_{c,i}\sin\phi_i}{\sqrt{1-\cos^2\psi_i\cos^2\phi_i}} & \frac{\sin\phi_i\cos\psi_i}{\sqrt{1-\cos^2\psi_i\cos^2\phi_i}} \end{bmatrix} \quad (4)$$

$$\boldsymbol{R}_i = \begin{bmatrix} 0 & 0 & -1 \\ \cos\beta_i & -\sin\beta_i & 0 \\ -\sin\beta_i & -\cos\beta_i & 0 \end{bmatrix} \quad (5)$$

The angles ϕ_i and ψ_i describing the relationship between the orbital velocity vectors of the two objects at the TCA can be computed from the expressions derived in [22] keeping in mind which satellite executes the manoeuvre. Furthermore, the angle β_i relates the auxiliary inertial reference frame $\langle x, y, z\rangle_i$ to the B-plane reference frame $\langle \xi, \eta, \zeta \rangle$. The definition of β_i is illustrated in Fig. 2a for the case in which satellite S_1 manoeuvres and in Fig. 2b for the case in which satellite S_2 manoeuvres. While for satellite S_1 the same definition as the one derived by Bombardelli in [22] is used, for satellite S_2 a new auxiliary inertial reference frame $\langle x, y, z\rangle_2$ is defined with the x-axis aligned with $\boldsymbol{v}_2$ instead of $\boldsymbol{v}_1$.

Finally, the relative position of the two satellites after executing the shared CAM can be determined by considering their respective displacements on the collision B-plane. Fig. 3 illustrates the pre- and post-manoeuvre conjunction geometries on the B-plane, assuming a predicted miss distance of $\boldsymbol{r}_0$ before the execution of the shared manoeuvre. Mathematically, the final relative position after the shared CAM can be computed as follows:

$$\begin{aligned} \Delta\boldsymbol{r}_f &= \boldsymbol{r}_1 - \boldsymbol{r}_2 = \\ &= \boldsymbol{r}_0 + \Delta\boldsymbol{r}_1 - \Delta\boldsymbol{r}_2 = \\ &= \boldsymbol{r}_0 + \boldsymbol{M}_1\Delta\boldsymbol{v}_1 - \boldsymbol{M}_2\Delta\boldsymbol{v}_2 \end{aligned} \quad (6)$$

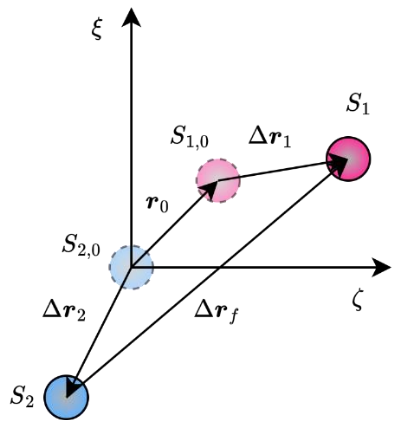

Fig. 3. S_1-S_2 relative position after the shared CAM

2.2. *Optimal Delta-V design of shared CAMs*

In this section, the optimal shared CAM that minimises propellant consumption is determined by formulating the problem as a NLP problem, subject to a geometric or probabilistic constraint. The impulsive CAMs for both satellites are limited to their respective along-track directions and are optimised for a specified manoeuvring time for each satellite, which may differ. The global optimum, taking into account the execution time of the manoeuvres, is subsequently identified using the methodology outlined in Section 2.4.

When formulating the NLP, it is more straightforward to initially consider three-dimensionally oriented impulsive CAMs and then reduce the dimensionality of the problem to derive an analytical solution. Since the objective is to minimise the total propellant consumption, the optimisation variable $\boldsymbol{x}$ is the manoeuvre impulses of the two satellites:

$$\boldsymbol{x} = (\Delta\boldsymbol{v}_1, \Delta\boldsymbol{v}_2) \tag{7}$$

where $\Delta\boldsymbol{v}_i = [\Delta v_r, \Delta v_\theta, \Delta v_h]_i^T$ is the manoeuvre impulse executed by S_i in its local RTN reference frame. Therefore, the objective function $f(\boldsymbol{x})$ is given by:

$$f(\boldsymbol{x}) = \Delta\boldsymbol{v}_1^T\Delta\boldsymbol{v}_1 + \Delta\boldsymbol{v}_2^T\Delta\boldsymbol{v}_2 \tag{8}$$

The nonlinear equality constraint $g(\boldsymbol{x})$ is defined as in [23]:

$$g(\boldsymbol{x}) = \Delta\boldsymbol{r}_f^T\boldsymbol{A}\Delta\boldsymbol{r}_f - \delta^2 \tag{9}$$

where $\Delta\boldsymbol{r}_f$ is the post-manoeuvre relative position at the TCA between the two satellites in B-plane coordinates, and the matrix $\boldsymbol{A}$ and scalar δ depend on the selected geometric or probabilistic constraint:

- Miss distance: $\boldsymbol{A} = \boldsymbol{I}, \quad \delta^2 = d^2$ (10)
- B-plane miss distance: $\boldsymbol{A} = \boldsymbol{Q}, \quad \delta^2 = d_{B,2D}^2$ (11)
- Mahalanobis distance: $\boldsymbol{A} = \boldsymbol{Q}^*, \quad \delta^2 = SMD$ (12)

Matrices $\boldsymbol{Q}$ and $\boldsymbol{Q}^*$ are defined as in [24]:

$$\boldsymbol{Q} = \begin{bmatrix} 1 & 0 & 0 \\ 0 & 0 & 0 \\ 0 & 0 & 1 \end{bmatrix}, \quad \boldsymbol{Q}^* = \begin{bmatrix} \frac{1}{\sigma_\xi^2} & 0 & -\frac{\rho_{\xi\zeta}}{\sigma_\xi\sigma_\zeta} \\ 0 & 0 & 0 \\ -\frac{\rho_{\xi\zeta}}{\sigma_\xi\sigma_\zeta} & 0 & \frac{1}{\sigma_\zeta^2} \end{bmatrix} \tag{13}$$

where σ_ξ, σ_ζ and $\rho_{\xi\zeta}$ can be extracted from the relative position covariance matrix in B-plane axes whose (ξ, ζ) submatrix reads:

$$\boldsymbol{C}_{\xi\zeta} = \begin{bmatrix} \sigma_\xi^2 & \rho_{\xi\zeta}\sigma_\xi\sigma_\zeta \\ \rho_{\xi\zeta}\sigma_\xi\sigma_\zeta & \sigma_\zeta^2 \end{bmatrix} \tag{14}$$

Operationally, the acceptable collision risk threshold is typically defined in terms of miss distance and collision probability. In the case of collision probability, the corresponding SMD threshold can be determined from Chan's method [25].

The equality constraint can be expressed in terms of the optimisation variable by substituting Eq. (6) into Eq. (9), resulting in:

$$\begin{aligned} g(\boldsymbol{x}) &= \Delta\boldsymbol{r}_f^T\boldsymbol{A}\Delta\boldsymbol{r}_f - \delta^2 = \\ &= \gamma_0 + 2\boldsymbol{r}_0^T\boldsymbol{A}\boldsymbol{M}_1\Delta\boldsymbol{v}_1 - 2\boldsymbol{r}_0^T\boldsymbol{A}\boldsymbol{M}_2\Delta\boldsymbol{v}_2 + \\ &\quad +\Delta\boldsymbol{v}_1^T\widetilde{\boldsymbol{A}}_{11}\Delta\boldsymbol{v}_1 + \Delta\boldsymbol{v}_2^T\widetilde{\boldsymbol{A}}_{22}\Delta\boldsymbol{v}_2 + \\ &\quad -2\Delta\boldsymbol{v}_1^T\widetilde{\boldsymbol{A}}_{12}\Delta\boldsymbol{v}_2 \end{aligned} \tag{15}$$

where the scalar term γ_0 and the matrix $\widetilde{\boldsymbol{A}}_{ij}$ are:

$$\gamma_0 = \boldsymbol{r}_0^T\boldsymbol{A}\boldsymbol{r}_0 - \delta^2 \tag{16}$$

$$\widetilde{\boldsymbol{A}}_{ij} = \boldsymbol{M}_i^T\boldsymbol{A}\boldsymbol{M}_j \tag{17}$$

Given the optimisation variable $\boldsymbol{x}$, the objective function $f(\boldsymbol{x})$, and the equality constraint $g(\boldsymbol{x})$, the optimal impulsive shared manoeuvre is obtained by solving the following NLP problem:

$$\min_{\boldsymbol{x}} f(\boldsymbol{x}) \quad \text{s.t.} \quad g(\boldsymbol{x}) = 0 \tag{18}$$

The solution of the constrained optimisation problem can be obtained using the method of Lagrange multipliers. The Lagrangian function associated with the problem is defined as:

$$\mathcal{L}(\boldsymbol{x}, \lambda) = f(\boldsymbol{x}) + \lambda g(\boldsymbol{x}) \tag{19}$$

where λ is the scalar Lagrange multiplier associated with the scalar equality constraint $g(\boldsymbol{x}) = 0$. The necessary condition for optimality, corresponding to the stationary points of $\mathcal{L}(\boldsymbol{x}, \lambda)$, is:

$$\nabla_{\boldsymbol{x},\lambda}\mathcal{L}(\boldsymbol{x}, \lambda) = 0 \Leftrightarrow \begin{cases} \nabla_{\boldsymbol{x}} f(\boldsymbol{x}) + \lambda \nabla_{\boldsymbol{x}} g(\boldsymbol{x}) = 0 \\ g(\boldsymbol{x}) = 0 \end{cases} \tag{20}$$

Substituting Eqs. (8) and (15) into Eq. (20) and simplifying, the necessary condition for optimality can be expressed in terms of the optimisation variables. This yields a system of seven coupled nonlinear equations (comprising two vector equations and one scalar equation) with seven unknowns ($\Delta\boldsymbol{v}_1, \Delta\boldsymbol{v}_2$ and λ), which can be solved numerically:

$$\begin{cases} \left(\boldsymbol{I} + \lambda\widetilde{\boldsymbol{A}}_{11}\right)\Delta\boldsymbol{v}_1 + \lambda\boldsymbol{b}_1 - \lambda\widetilde{\boldsymbol{A}}_{12}\Delta\boldsymbol{v}_2 = 0 \\ \left(\boldsymbol{I} + \lambda\widetilde{\boldsymbol{A}}_{22}\right)\Delta\boldsymbol{v}_2 - \lambda\boldsymbol{b}_2 - \lambda\widetilde{\boldsymbol{A}}_{12}\Delta\boldsymbol{v}_1 = 0 \\ \gamma_0 + 2\boldsymbol{b}_1^T\Delta\boldsymbol{v}_1 - 2\boldsymbol{b}_2^T\Delta\boldsymbol{v}_2 + \Delta\boldsymbol{v}_1^T\widetilde{\boldsymbol{A}}_{11}\Delta\boldsymbol{v}_1 + \\ \quad + \Delta\boldsymbol{v}_2^T\widetilde{\boldsymbol{A}}_{22}\Delta\boldsymbol{v}_2 - 2\Delta\boldsymbol{v}_1^T\widetilde{\boldsymbol{A}}_{12}\Delta\boldsymbol{v}_2 = 0 \end{cases} \tag{21}$$

where:

$$\boldsymbol{b}_i = \boldsymbol{M}_i^T\boldsymbol{A}\boldsymbol{r}_0 \tag{22}$$

Assuming a reasonable simplification where each satellite performs manoeuvres strictly in its along-track direction, i.e. $\Delta\boldsymbol{v}_i = [0, \Delta v_i, 0]^T$, as is typically the case in collision avoidance operations, the problem reduces from seven to three unknowns, requiring only three equations to find the solution. For simplicity, the 2nd and 5th equations from the system in Eq. (21) are selected, resulting in a system of three scalar equations with three scalar unknowns ($\Delta v_1, \Delta v_2$ and λ), formalised as follows:

$$\begin{cases} (1 + \lambda\tilde{a}_{11})\Delta v_1 + \lambda b_1 - \lambda\tilde{a}_{12}\Delta v_2 = 0 \\ (1 + \lambda\tilde{a}_{22})\Delta v_2 - \lambda b_2 - \lambda\tilde{a}_{12}\Delta v_1 = 0 \\ \gamma_0 + 2b_1\Delta v_1 - 2b_2\Delta v_2 + \tilde{a}_{11}\Delta v_1^2 + \\ \quad + \tilde{a}_{22}\Delta v_2^2 - 2\tilde{a}_{12}\Delta v_1\Delta v_2 = 0 \end{cases} \tag{23}$$

where $\tilde{a}_{11}$, $\tilde{a}_{22}$ and $\tilde{a}_{12}$ are the central diagonal elements of the matrices $\widetilde{\boldsymbol{A}}_{11}$, $\widetilde{\boldsymbol{A}}_{22}$ and $\widetilde{\boldsymbol{A}}_{12}$, respectively, and b_1 and b_2 refer to the central components of the vectors $\boldsymbol{b}_1$ and $\boldsymbol{b}_2$, respectively.

The previous system of equations can be further reduced to a single fourth-order equation in λ, which can be solved analytically. Once λ is determined, it can be used to compute the along-track impulsive CAMs for both satellites, as provided by the following equations:

$$\Delta v_1 = \frac{-\lambda(b_1 + \tilde{a}_{22}b_1\lambda - \tilde{a}_{12}b_2\lambda)}{\tilde{a}_{11}\lambda + \tilde{a}_{22}\lambda - \tilde{a}_{12}^2\lambda^2 + \tilde{a}_{11}\tilde{a}_{22}\lambda^2 + 1} \tag{24}$$

$$\Delta v_2 = \frac{\lambda(b_2 + \tilde{a}_{11}b_2\lambda - \tilde{a}_{12}b_1\lambda)}{\tilde{a}_{11}\lambda + \tilde{a}_{22}\lambda - \tilde{a}_{12}^2\lambda^2 + \tilde{a}_{11}\tilde{a}_{22}\lambda^2 + 1} \tag{25}$$

2.3. Fair design of shared CAMs

In this section, a novel methodology is introduced for designing a shared CAM that distributes manoeuvre effort based on each satellite's contribution to the collision risk. This approach offers significant benefits for STM, promoting the sustainable and responsible use of space while encouraging international cooperation by facilitating coordination between satellite O/Os in agreeing on the CAM to be executed. For this method to be successful, it must ensure fairness for all parties involved. To this aim, it is assumed that the satellite executing the larger manoeuvre —and thus consuming more propellant— should be the one contributing more to the collision risk. The concept of fairness has been integrated into the optimisation of the shared CAM through a fairness factor η that balances the control effort between both satellites.

In collision avoidance operations, the state-of-the-art method for estimating collision risk relies on a probabilistic metric known as the probability of collision. This metric depends not only on the relative position between the satellites but also on the combined HBR, which models their combined size, and the state covariance, which accounts for the uncertainty in their orbital information. While more complex formulations of the fairness factor could be developed for the optimal design of a shared CAM, for demonstration purposes, the contributions to this fairness factor are defined using the following dimensionless quantities, which depend on the objects' size and orbital uncertainty, respectively:

$$\eta = \eta_s = \frac{HBR_2}{HBR_1}, \qquad \eta = \eta_u = \frac{\mathrm{tr}(\boldsymbol{C}_2)}{\mathrm{tr}(\boldsymbol{C}_1)} \tag{26}$$

where $\mathrm{tr}(\boldsymbol{C}_i)$ is the trace of the position covariance matrix of satellite S_i.

These contributions to the fairness factor can encourage satellite O/Os to adopt practices that promote the sustainability of the space environment, primarily by reducing orbital uncertainty. This can be accomplished through various means, such as improving the quality and quantity of sensor observations with advanced sensor technologies, encouraging data sharing among different stakeholders in space activities, and designing satellites with materials and structures that are more easily detectable by SST sensors. However, since larger satellites inherently pose a greater collision risk, it is crucial to achieve a delicate equilibrium when defining the fairness factor. A possible definition of the fairness factor that simultaneously considers both satellite size and orbital uncertainty is:

$$\eta = \eta_s \eta_u = \frac{HBR_2}{HBR_1}\frac{\mathrm{tr}(\boldsymbol{C}_2)}{\mathrm{tr}(\boldsymbol{C}_1)} \tag{27}$$

Once the fairness factor is defined, it must be incorporated into the formulation of the NLP problem to optimise the fair shared CAM. Since both satellites execute impulsive manoeuvres strictly in their respective along-track directions (which do not need to occur simultaneously), the manoeuvre impulses can be expressed in terms of the fairness factor as follows:

$$\Delta\boldsymbol{v}_1 = [0, \Delta v, 0]^T = \Delta\boldsymbol{v} \tag{28}$$

$$\Delta\boldsymbol{v}_2 = [0, \pm\eta\Delta v, 0]^T = \pm\eta\Delta\boldsymbol{v} \tag{29}$$

where the manoeuvre impulse for each satellite is defined in its respective RTN reference frame. The $\pm$ sign in front of the fairness factor accounts for all possible combinations of manoeuvre directions: both satellites executing the CAM in either their positive or negative along-track directions, or one satellite executing the CAM in its positive along-track direction while the other in its negative along-track direction.

Since the new optimisation variable is a scalar, specifically $x = \Delta v$, the NLP problem can be reformulated with the objective function defined as follows:

$$f(x) = \Delta\boldsymbol{v}_1^T\Delta\boldsymbol{v}_1 + \Delta\boldsymbol{v}_2^T\Delta\boldsymbol{v}_2 = (1+\eta^2)\Delta v^2 \tag{30}$$

The nonlinear equality constraint $g(x)$ is then expressed as:

$$\begin{aligned} g(x) &= \Delta\boldsymbol{r}_f^T\boldsymbol{A}\Delta\boldsymbol{r}_f - \delta^2 = \\ &= \gamma_0 + 2\boldsymbol{r}_0^T\boldsymbol{A}\boldsymbol{M}_\eta\Delta\boldsymbol{v} + \Delta\boldsymbol{v}^T\boldsymbol{M}_\eta^T\boldsymbol{A}\boldsymbol{M}_\eta\Delta\boldsymbol{v} = \\ &= \gamma_0 + 2\boldsymbol{b}_\eta\Delta\boldsymbol{v} + \Delta\boldsymbol{v}^T\boldsymbol{A}_\eta\Delta\boldsymbol{v} \end{aligned} \tag{31}$$

where the following auxiliary variables are used:

$$\gamma_0 = \boldsymbol{r}_0^T\boldsymbol{A}\boldsymbol{r}_0 - \delta^2 \tag{32}$$

$$\boldsymbol{M}_\eta = \boldsymbol{M}_1 \mp \eta\boldsymbol{M}_2 \tag{33}$$

$$\boldsymbol{A}_\eta = \boldsymbol{M}_\eta^T\boldsymbol{A}\boldsymbol{M}_\eta \tag{34}$$

$$\boldsymbol{b}_\eta = \boldsymbol{r}_0^T\boldsymbol{A}\boldsymbol{M}_\eta \tag{35}$$

Finally, it is convenient to express Eq. (31) solely in terms of scalar quantities, resulting in:

$$g(x) = a_\eta\Delta v^2 + 2b_\eta\Delta v + \gamma_0 \tag{36}$$

where a_η is the second element of the main diagonal of $\boldsymbol{A}_\eta$, and b_η is the second component of $\boldsymbol{b}_\eta$.

The Lagrangian function and the necessary condition for optimality can be derived from Eqs. (30) and (36). Notably, the problem simplifies to finding the derivative of the Lagrangian function with respect to λ, which involves solving the equation $g(x) = 0$. Consequently, the optimal manoeuvre impulse is determined by solving the following second-order equation:

$$\Delta v = \frac{-b_\eta \pm \sqrt{b_\eta^2 - a_\eta\gamma_0}}{a_\eta} \tag{37}$$

This approach may yield two distinct solutions. The optimal solution is the one that minimises the objective function given in Eq. (30), specifically the solution with the smallest $|\Delta v|$. The optimal solution can be either positive or negative, indicating that the manoeuvre impulse is directed either in the positive along-track direction or in the opposite direction.

2.4. Temporal optimisation of shared CAMs

Sections 2.2 and 2.3 have introduced two NLP formulations for optimising a shared CAM: one focusing exclusively on global propellant efficiency, and another that incorporates a fair distribution of manoeuvring effort according to each satellite's contribution to the collision risk. These NLP problems are solved for specified manoeuvring times for both satellites, which do not need to occur simultaneously. To determine the optimal combination of manoeuvres for both satellites, a parametric analysis must be performed on the timing of each satellite's impulsive CAM execution. The search space for the optimal solution is defined as follows:

$$\theta_{m,i}^k = \theta_{c,i} - k\Delta\theta_i\,, \qquad k = 1, \ldots, N \tag{38}$$

Moreover, the identification of the globally optimal shared CAM is achieved using a newly defined objective function that simultaneously considers both total propellant consumption and the timing of manoeuvres relative to the TCA. This definition of the objective function also allows to minimise the time the satellite is out of its operational orbit. The optimisation variables in Eq. (39) are non-dimensional to ensure they contribute equally to the overall cost function:

$$J = w_1(\Delta\bar{v}_1^2 + \Delta\bar{v}_2^2) + w_2 \frac{\Delta\bar{t}_1 + \Delta\bar{t}_2}{2} \tag{39}$$

where $\Delta\bar{v}_1$ and $\Delta\bar{v}_2$ are the manoeuvre impulses determined by the NLP problem, non-dimensionalised by a reference velocity $v_{ref} = 100$ mm/s, and $\Delta\bar{t}_1$ and $\Delta\bar{t}_2$ are the corresponding lead times of the manoeuvres relative to the TCA, non-dimensionalised by a reference time $t_{ref} = 1$ h. The weighting factors w_1 and w_2 determine the relative importance of propellant consumption versus manoeuvre lead time.

The global objective function specified in Eq. (39) is formulated with a focus on practical operational considerations. Satellite operators typically prefer to delay a CAM until closer to the TCA to reduce the uncertainty in collision risk prediction. New sensor observations during this period may reveal that the collision risk has fallen below the acceptable threshold, thereby eliminating the need for a manoeuvre and allowing the satellite to continue its normal operations. However, this strategy comes at the cost of increased propellant consumption, as larger manoeuvres are necessary to mitigate collision risk when executed closer to the TCA. Propellant consumption is a critical concern for satellite operators, as it directly affects the satellite's operational lifetime. Consequently, CAM lead time and propellant consumption are incorporated into the global objective function formulation, which aims to balance these factors effectively according to various optimisation strategies. The three different CAM optimisation strategies considered in this work are:

- **Propellant**: it focuses exclusively on minimising propellant consumption, without regard for the lead time relative to the TCA. It is suited for scenarios where propellant is limited and collision risk tolerance is low.

- **Lead Time**: this approach aims to delay manoeuvres as much as possible, disregarding the associated increase in propellant consumption. It seeks to minimise the time the satellite spends outside its operational orbit and may ultimately result in a conjunction resolution that does not necessitate a CAM, thanks to new sensor observations and reduced orbital uncertainty.

- **Balanced**: this strategy seeks to find a compromise between minimising propellant consumption and delaying the timing of the manoeuvre to as close to the TCA as possible.

The weighting factors associated with each CAM optimisation strategy are provided in Table 1:

Table 1. Weighting factors for the optimisation strategies

Optimisation strategy	w_1	w_2
Propellant	1	0
Lead time	0	1
Balanced	0.5	0.5

The algorithm applied to compute the optimal shared CAM considering both the results of the NLP problem and the global objective function J depending on the selected optimisation strategy is provided in Algorithm 1 below.

Algorithm 1: Shared CAM optimisation

Inputs: $\boldsymbol{r}_i$, $\boldsymbol{v}_i$, $\boldsymbol{C}_i$, HBR_i, $\Delta v_{i,max}$, δ, $\Delta\theta_i$, N, w_1, w_2
Outputs: Δv_i

Get $\theta_{c,i}$ from $\boldsymbol{r}_i$ and $\boldsymbol{v}_i$
Compute $\boldsymbol{\theta}_{m,i}$
Compute $\boldsymbol{A}$ according to δ
for $\theta_{m,1}$ in $\boldsymbol{\theta}_{m,1}$ **do**
  for $\theta_{m,2}$ in $\boldsymbol{\theta}_{m,2}$ **do**
    Compute $\boldsymbol{M}_i$
    Solve the NLP problem: get Δv_i
    if $\Delta v_i < \Delta v_{i,max}$ **then**
      Compute J
    end if
  end for
end for
Find J_{min}
Get Δv_i associated with J_{min}

3. Results and discussion

This section presents the analysis of a real close encounter between two active manoeuvrable satellites. Firstly, the main orbital and conjunction parameters are detailed, including the state and position covariance of both objects at the TCA, their HBR, the predicted miss distance and the probability of collision. Based on these parameters, the different formulations of the fairness factor introduced in Section 2.3 are computed, providing insights into the potential outcomes of each approach. Subsequently, the fair shared CAM strategy is applied to resolve the conjunction for two representative fairness factors. Finally, the performance of the fair shared CAM is compared against both the individual CAM executed by a single satellite and the propellant-optimal shared CAM.

The real conjunction examined in this section involves the following two manoeuvrable satellites: Starlink 3173, part of SpaceX's mega-constellation, and Taijing 2-04, an optical remote sensing satellite. The relevant information for both satellites is summarised in Table 2, including the HBRs, which were obtained from the DISCOS database [26].

Table 2. Satellites general information

Satellite name	COSPAR ID	HBR [m]
Starlink 3173	2022-005H	4.43
Taijing 2-04	2024-016D	3

The orbital information for both objects is obtained from their respective Two-Line Elements (TLEs), retrieved from Space-Track [27]. These orbits are then propagated forward in time, revealing a high-risk close approach between the satellites. The predicted TCA and the baseline collision risk metrics are presented in Table 3 below.

Table 3. Baseline conjunction parameters

TCA	d [m]	PoC [-]
2024-01-30 18:53:48.20	140.94	2.099×10^{-3}

The orbital state and the associated uncertainty of both satellites at the TCA are reported below. The state is expressed in the J2000 reference frame, while the position uncertainty is provided in the local RTN reference frame of each satellite. The position uncertainty associated with both satellites' orbital information is estimated using an abacus developed from GMV's experience, which takes into account the time elapsed since the last orbit determination. The state and position uncertainty at the TCA for the satellite Starlink 3173 are:

$$\begin{aligned} \boldsymbol{r}_1 &= [2145.13,\ -5396.83,\ 3749.83]^T \text{ km} \\ \boldsymbol{v}_1 &= [6.094,\ -0.702,\ -4.481]^T \text{ km/s} \\ \boldsymbol{\sigma}_{RTN,1} &= [2.425,\ 1167.06,\ 8.372]^T \text{ m} \end{aligned} \tag{40}$$

while the corresponding orbital information for the satellite Taijing 2-04 is:

$$\begin{aligned} \boldsymbol{r}_2 &= [2145.07,\ -5396.78,\ 3749.94]^T \text{ km} \\ \boldsymbol{v}_2 &= [0.385,\ -4.224,\ -6.297]^T \text{ km/s} \\ \boldsymbol{\sigma}_{RTN,2} &= [2.109,\ 1131.61,\ 8.270]^T \text{ m} \end{aligned} \tag{41}$$

With these orbital and physical characteristics of both satellites, the different formulations of the fairness factor presented in Section 2.3 are computed. The results are detailed in Table 4.

Table 4. Results for different fairness factor formulations

$\eta = \eta_s$	$\eta = \eta_u$	$\eta = \eta_s \eta_u$
0.68	0.94	0.64

After presenting the results for the various fairness factor formulations proposed in this study, it is interesting to compare the two shared CAM strategies discussed in previous sections: the fair shared CAM and the propellant-optimal shared CAM. To this end, the collision risk associated with the close approach between Starlink 3173 and Taijing 2-04 is mitigated using a fair shared CAM, employing two representative fairness factors to illustrate their impact on the fair distribution of manoeuvring effort. The same conjunction is then analysed using the propellant-optimal shared CAM for comparative purposes. For simplicity, the collision risk metric considered is the B-plane miss distance, with a post-CAM threshold of 1.5 km.

Regarding the fair shared CAM, a fairness factor of $\eta = 0.05$ is initially used, indicating that satellite S_1 significantly contributes to the collision risk and, consequently, should bear the majority of the manoeuvring costs. The results of this analysis are depicted in Fig. 4, where the Δv of both satellites is shown across various combinations of manoeuvring times. The optimal solutions identified for the three CAM optimisation strategies —propellant, lead time and balanced— are also highlighted. Additionally, the maximum manoeuvre Δv that the satellites' propulsion systems can provide, assumed to be 50 mm/s for both satellites, is indicated. An equivalent sensitivity analysis is conducted in Fig. 5 using a more balanced fairness factor of $\eta = 0.7$, which aligns with the fairness factor obtained when only the HBRs of the satellites are considered. This fairness factor, being closer to 1, results in a more equitable distribution of manoeuvring costs, with satellite S_2 being required to contribute slightly more towards mitigating the collision risk. Finally, Fig. 6 presents the results obtained using the propellant-centred formulation of the shared CAM optimisation problem, where the manoeuvre impulses are independently optimised to minimise total propellant consumption, without considering the fair distribution of manoeuvring costs.

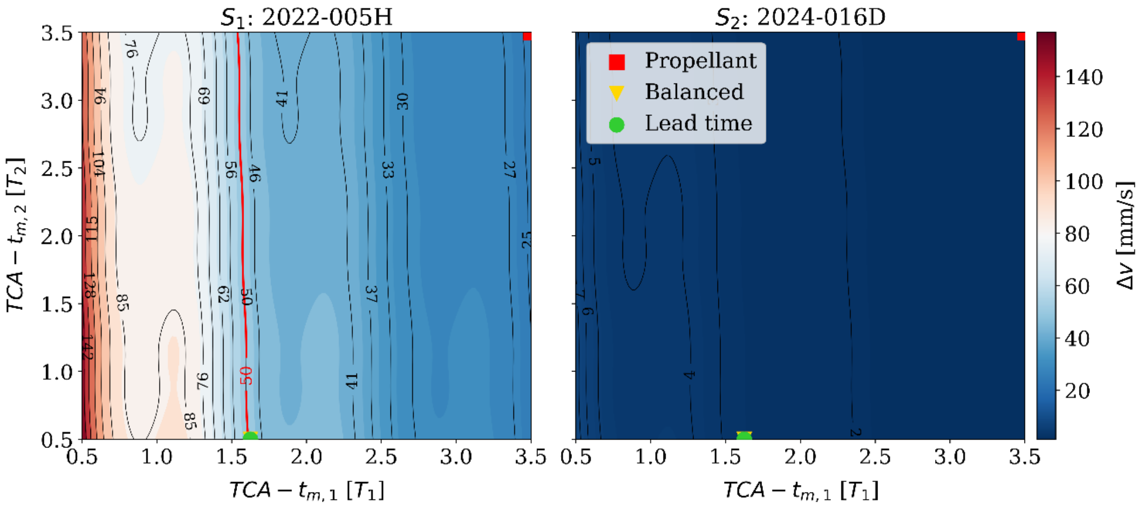

Fig. 4. Fair shared CAM for $\eta = 0.05$

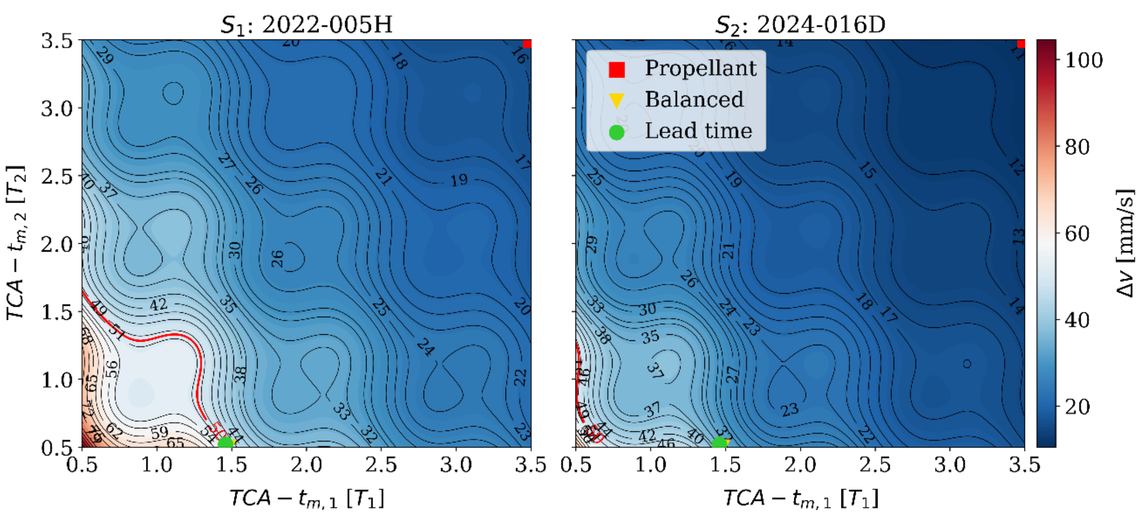

Fig. 5. Fair shared CAM for $\eta = 0.7$

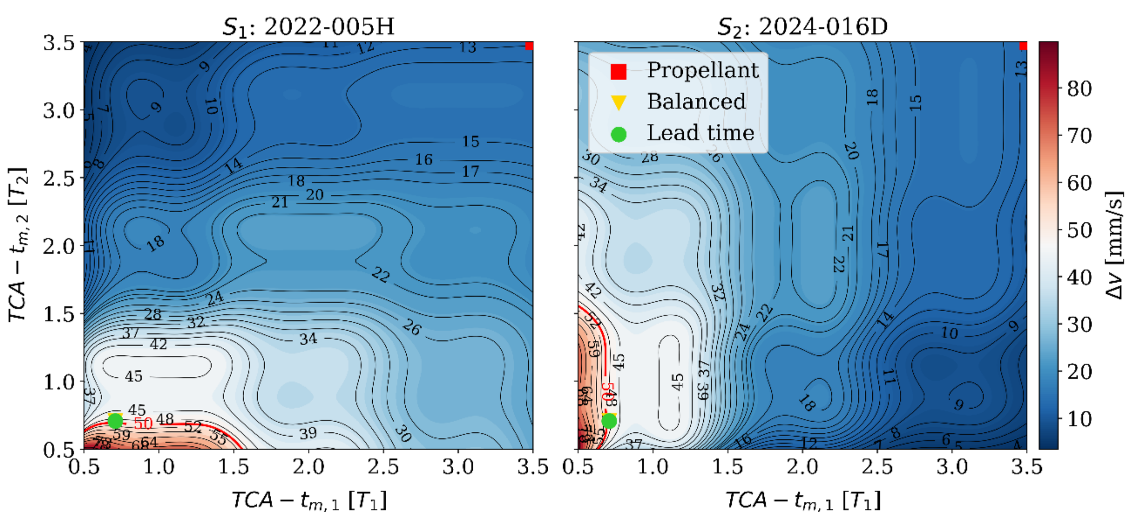

Fig. 6. Propellant-optimal shared CAM

The impact of the fairness factor is immediately evident in Fig. 4 and Fig. 5, where the optimal Δv's for satellite S_1 are consistently higher than those for satellite S_2, reflecting S_2's lower contribution to the collision risk and its consequent reward in the form of reduced manoeuvring costs. Conversely, Fig. 6 shows that the optimisation strategy focused solely on minimising total propellant consumption might result in an equitable distribution of manoeuvring costs when the manoeuvre times are similar. However, when the manoeuvre times differ, the satellite that executes its manoeuvre earlier compensates with a higher Δv to counterbalance the reduced effect of the manoeuvre executed by the satellite that delays its action. This dynamic could lead to a situation where both O/Os might compete to delay their manoeuvre, potentially resulting in scenarios where neither an individual nor a shared CAM can sufficiently mitigate the collision risk. Alternatively, it might force the operator with a greater concern for collision risk to unilaterally execute the CAM, a situation commonly observed in current operational practices with individual CAMs.

With regard to the CAM optimisation strategy, the propellant-minimisation approach favours the earliest possible manoeuvre times. This allows the manoeuvre's effect on the orbital position to accumulate over several revolutions, resulting in greater separation by the TCA. In contrast, the lead time and balanced strategies yield results closer to the Δv limit of the propulsion system. Another advantage of the shared CAM strategy for mitigating collision risk, compared to an individual CAM, is evident from these analyses. With a fairness factor of $\eta = 0.7$, which promotes a more balanced distribution of manoeuvring effort, satellite S_1 has greater flexibility to delay its manoeuvre. In contrast, with $\eta = 0.05$, where satellite S_1 receives minimal contribution from S_2, feasible solutions are not available beyond 1.6 orbital revolutions before TCA. Thus, the shared CAM strategy allows for the postponement of the mitigation action, providing an opportunity for new sensor observations and reduced uncertainty to potentially render the manoeuvre unnecessary.

Another relevant analysis involves comparing the shared CAM strategies with the individual CAM approach, the traditional operational strategy for mitigating collision risk, where a single satellite assumes the entire manoeuvring costs. Fig. 7, Fig. 8 and Fig. 9 illustrate the comparison between the Δv required by the shared manoeuvre optimal solutions and that of the individual CAM scenario. These figures depict the savings each satellite achieves relative to the scenario where it undertakes the entire manoeuvre effort itself, expressed as the percentage difference between the two solutions. As expected, the difference is consistently greater than zero across all cases, indicating that sharing the manoeuvre cost between the two satellites is always advantageous.

Focusing on the fair shared CAM, when the contribution of each satellite to the collision risk is highly unbalanced, as in Fig. 7, the comparison with the individual CAM shows that the satellite contributing significantly more to the collision risk can achieve Δv savings of up to 20% relative to the individual CAM, while the other satellite can save over 80%. In cases where the contribution to collision risk is more balanced, as in Fig. 8 for $\eta = 0.7$, both satellites benefit from propellant savings of more than 70% when the manoeuvring times differ significantly, and savings between 40% and 60% when they perform the manoeuvres at similar times. The results presented in Fig. 6 for the propellant-optimal shared CAM exhibit symmetric behaviour with respect to the timing of the manoeuvres, with both satellites achieving nearly 50% savings when the manoeuvres are executed at similar times.

Finally, it is valuable to compare the two shared CAM strategies discussed in this study: the fair shared CAM, which allocates manoeuvring costs equitably based on each satellite's contribution to the collision risk, and the propellant-optimal shared CAM, which aims solely at minimising total propellant consumption without considering fairness. The results are presented in Fig. 10. for two different fairness factors used in the computation of the optimal fair shared CAM.

The results clearly demonstrate that the propellant-optimal shared CAM consistently yields the most propellant-efficient outcome. For $\eta = 0.05$, the largest discrepancy between the two strategies occurs when satellite S_1 executes its manoeuvre close to the TCA. This is because the fair manoeuvre penalises S_1 as the major contributor to the collision risk, while the propellant-optimal approach increases the Δv of the satellite that manoeuvres earlier. Consequently, the fair manoeuvre benefits satellite S_2, while the propellant-optimal solution leverages its flexibility to assign a larger manoeuvre to S_2, significantly enhancing the overall optimisation result. Conversely, both strategies exhibit similar performance when the satellite penalised in the fair approach manoeuvres early and the one rewarded manoeuvres close to the TCA. Consistent results are also obtained for $\eta = 0.7$, where both strategies perform similarly when the satellites manoeuvre at similar times. Overall, the additional benefits provided by the fairness factor —such as promoting the sustainable and responsible use of space and garnering support from international O/Os— tip the balance in favour of adopting the fair shared CAM strategy.

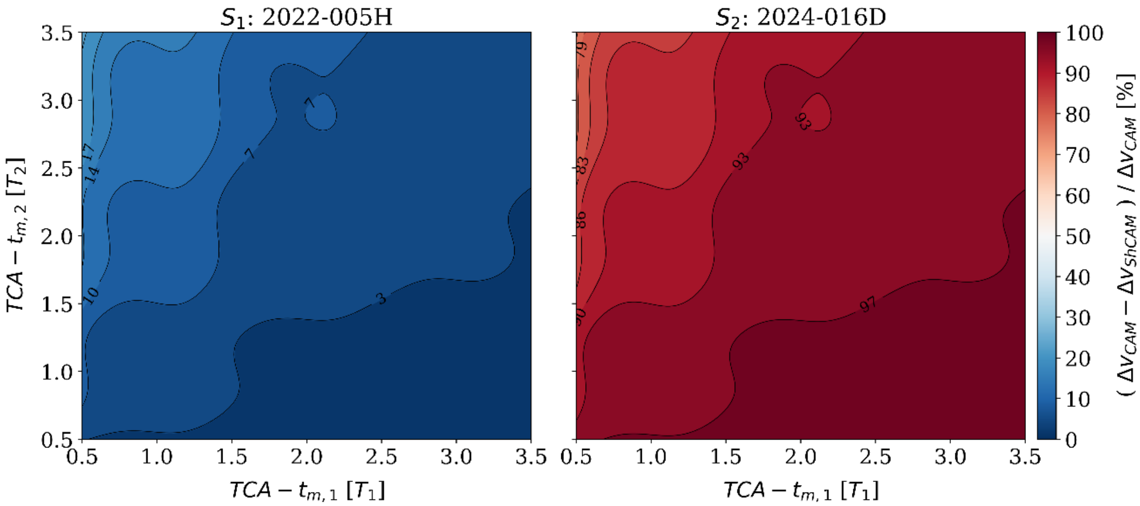

Fig. 7. Comparison between the fair shared CAM (η = 0.05) and the individual CAM

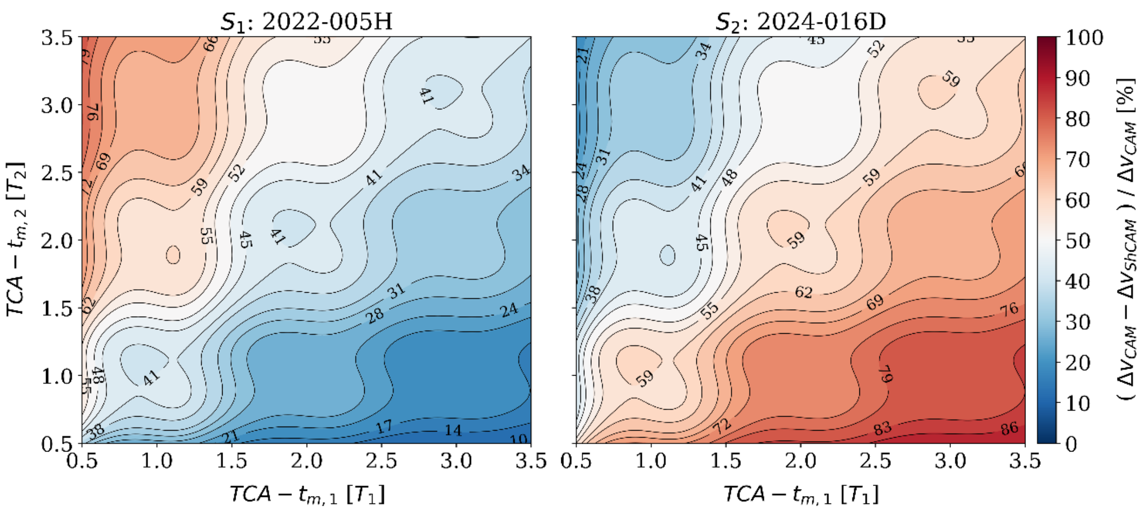

Fig. 8. Comparison between the fair shared CAM (η = 0.7) and the individual CAM

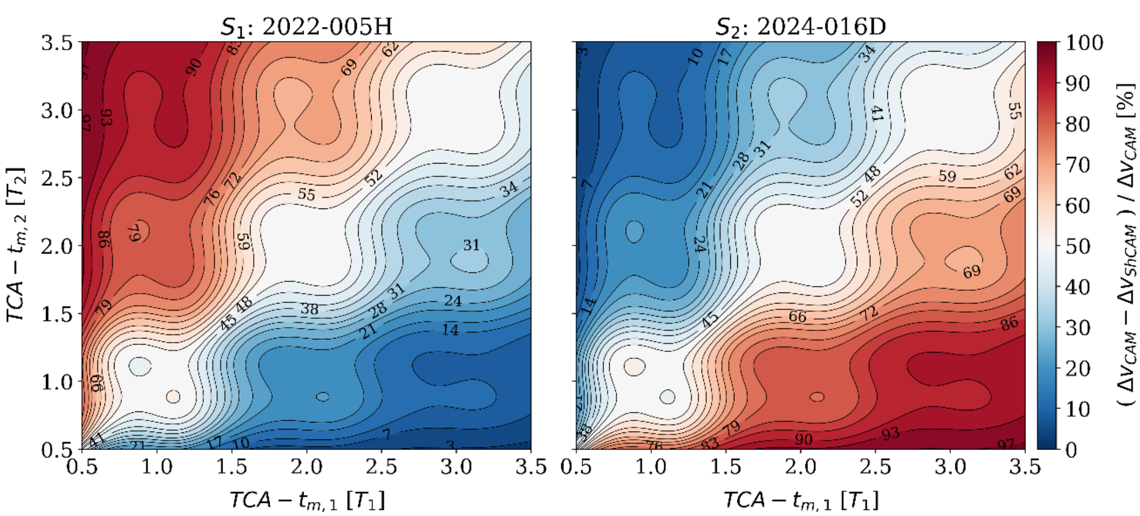

Fig. 9. Comparison between the propellant-optimal shared CAM and the individual CAM

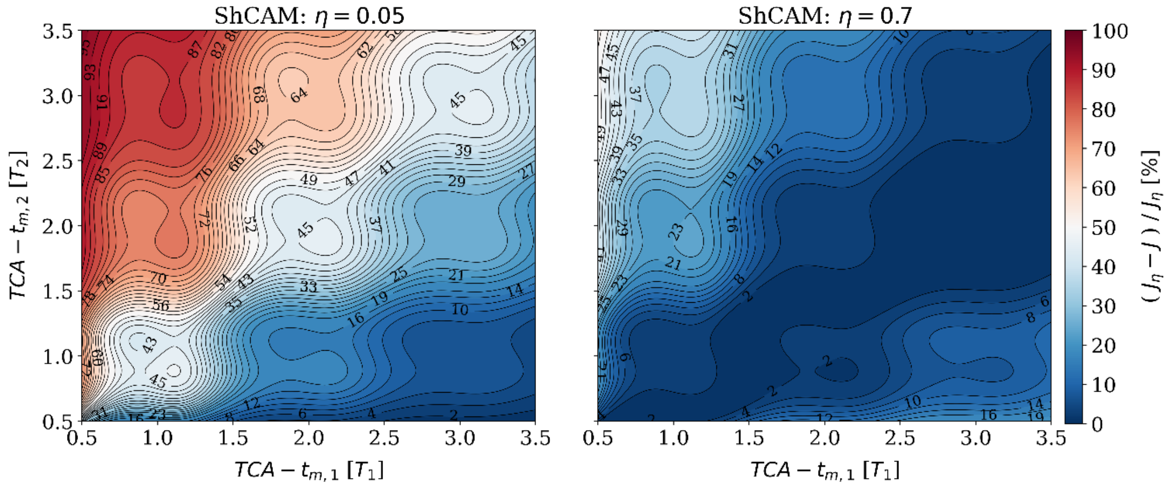

Fig. 10. Comparison between the fair and propellant-optimal shared CAMs (propellant strategy)

4. Conclusions

In the context of an increasingly congested space environment, this work aims to advance the development of strategies for the safe and efficient management of space traffic. Specifically, it introduces a novel methodology for designing and optimising shared CAMs. This strategy is intended to mitigate the collision risk associated with high-risk close approaches between active manoeuvrable satellites by implementing coordinated manoeuvres that reduce the collision risk metric to below a predefined acceptable threshold. Two distinct formulations are examined for comparative purposes: the fair shared CAM, which distributes manoeuvring costs fairly based on each satellite's contribution to the collision risk, and the propellant-optimal shared CAM, which minimises total propellant consumption without regard to the fair distribution of manoeuvring effort.

The analysis of a real conjunction event between two manoeuvrable satellites has demonstrated that the fair shared CAM is an effective strategy in terms of both collision risk mitigation and propellant consumption. Although it is suboptimal compared to the propellant-optimal shared CAM, the differences are not significant when the satellite penalised by the fair approach manoeuvres earlier and the one rewarded manoeuvres close to the TCA. Additionally, the fair shared CAM ensures an equitable distribution of manoeuvring costs, which discourages operators from delaying their decisions until close to the TCA in order to shift a greater portion of the manoeuvring burden onto the other operator. Furthermore, the shared CAM strategy facilitates the deferral of manoeuvres, as the combined effect of coordinated CAMs is more significant at the TCA than that of a single CAM. This approach allows for the receipt of new sensor measurements and, coupled with the inherent reduction in orbital uncertainty as the TCA approaches, may potentially render the manoeuvre unnecessary.

In conclusion, the shared CAM is demonstrated to be operationally viable, even with the simplifying assumptions applied in this study to facilitate closed-form analytical solutions and enable rapid evaluation of various optimisation strategies. Its inherent simplicity and flexibility —such as accommodating multiple criteria for defining the fairness factor— make it a promising strategy within the framework of future STM regulations. The design concept of the fair shared CAM encourages responsible satellite design and operations, and is particularly attractive to satellite O/Os due to its propellant savings compared to the traditional individual CAM approach.

Acknowledgements

This project has received funding from the “Comunidad de Madrid” under the “Ayudas destinadas a la realización de doctorados industriales” program (project IND2023/TIC-28739).

References

[1] European Space Agency, “Space debris by the numbers”, *ESA website*. [Online]. Available: https://www.esa.int/Space_Safety/Space_Debris/Space_debris_by_the_numbers. [Accessed: Aug. 26, 2024].

[2] D. J. Kessler and B. G. Cour-Palais, "Collision frequency of artificial satellites: The creation of a debris belt", *Journal of Geophysical Research: Space Physics*, vol. 83, pp. 2637–2646, 1978.

[3] European Space Agency Space Debris Office, "ESA's Annual Space Environment Report 2024", European Space Operations Centre (ESOC), GEN-DB-LOG-00288-OPS-SD, Darmstadt, Germany, Jul. 2024.

[4] J. McDowell, "Jonathan's Space Pages: Starlink Statistics", *Jonathan's Space Report*. [Online]. Available: https://planet4589.org/space/con/star/stats.html. [Accessed: Aug. 22, 2024].

[5] E. Kulu, "NewSpace Constellations", *NewSpace Index*. [Online]. Available: https://www.newspace.im/. [Accessed: Aug. 12, 2024].

[6] T. Pultarova and E. Howell, "Starlink satellites: Facts, tracking and impact on astronomy", [Online]. Available: https://www.space.com/spacex-starlink-satellites.html. [Accessed: Aug. 12, 2024].

[7] Eutelsat OneWeb, "Our Network", *oneweb.net*. [Online]. Available: https://oneweb.net/our-network. [Accessed: Aug. 12, 2024].

[8] A. Jones, "China is developing plans for a 13,000-satellite megaconstellation", *SpaceNews.com*. [Online]. Available: https://spacenews.com/china-is-developing-plans-for-a-13000-satellite-communications-megaconstellation/. [Accessed: Aug. 12, 2024].

[9] T. Kohnstamm, "Everything you need to know about Project Kuiper, Amazon's satellite broadband network", *Amazon.com*. [Online]. Available: https://www.aboutamazon.com/news/innovation-at-amazon/what-is-amazon-project-kuiper [Accessed: Aug. 12, 2024].

[10] European Space Agency, "ESA spacecraft dodges large constellation", *ESA website*. [Online]. Available: https://www.esa.int/Space_Safety/ESA_spacecraft_dodges_large_constellation. [Accessed: Aug. 14, 2024].

[11] J. Foust, "India's Chandrayaan-2 maneuvered to avoid close approach to NASA's Lunar Reconnaissance Orbiter", *SpaceNews.com*. [Online]. Available: https://spacenews.com/indias-chandrayaan-2-maneuvered-to-avoid-close-approach-to-nasas-lunar-reconnaissance-orbiter/. [Accessed: Aug. 14, 2024].

[12] C. Lan, "The Starlink-China Space Station near-collision: Questions, solutions, and an opportunity", *The Space Review*. [Online]. Available: https://thespacereview.com/article/4338/1. [Accessed: Aug. 14, 2024].

[13] S. A. Kaiser, "Rules of the Road for Space Traffic" in *Proceedings of the 46th IISL Colloquium on the Law of Outer Space*, Bremen, Germany, Sep. 2003, pp. 351-359.

[14] S. Nag, D. D. Murakami, M. T. Lifson, J. V. Cabrera, and P. H. Kopardekar, "A Concept for Civil Space Traffic Management" in *Small Satellite Conference*, Aug. 2018.

[15] S. Nag, D. Murakami, M. Lifson, and P. Kopardekar, "System autonomy for space traffic management" in *2018 IEEE/AIAA 37th Digital Avionics Systems Conference (DASC)*, Sep. 2018, pp. 1-10.

[16] Space Safety Coalition (SSC), *Best Practices for the Sustainability of Space Operations*, version 2.38, [Online]. Available: https://spacesafety.org/ [Accessed: Aug. 27, 2024].

[17] M. Borowitz, B. C. Gunter, M. Birch, and R. J. Macke, "An investigation into potential collision maneuver guidelines for future Space Traffic Management" in *Proceedings of the 22nd Advanced Maui Optical and Space Surveillance Technologies Conference (AMOS 2021)*, 2021.

[18] M. Michel and R. Bertrand, "Assessment of inter-operator rule-based collision avoidance operations" in *Proceedings of the 8th European Conference on Space Debris*, Apr. 2021.

[19] S. Burgis, P. Lenhardt, R. Bertrand, E. Farahvashi, J. Radtke, and C. Kebschull, "Enabling efficient satellite mission design with rule-based collision avoidance", *Journal of Space Safety Engineering*, 2024.

[20] V. Schaus et al., "First results of ESA's collision risk estimation and automated mitigation (CREAM) programme" in *Proceedings of the 73rd International Astronautical Congress (IAC-2022)*, Sep. 2022.

[21] C. Venigalla and D. J. Scheeres, "Cooperative and Non-Cooperative Approaches to Optimal Spacecraft Collision Avoidance" in *AIAA SCITECH 2022 Forum*, p. 1274, 2022.

[22] C. Bombardelli, “Analytical formulation of impulsive collision avoidance dynamics”, *Celestial Mechanics and Dynamical Astronomy*, vol. 118, pp. 99-114, 2014.

[23] S. Longoni, “Collision Avoidance Manoeuvres with Return Strategy in Earth and Cislunar Environment”, Master’s thesis, Politecnico di Milano, Milano, Italy, 2023.

[24] C. Bombardelli and J. Hernando-Ayuso, “Optimal impulsive collision avoidance in low earth orbit”, *Journal of Guidance, Control, and Dynamics*, vol. 38, no. 2, pp. 217-225, 2015.

[25] F. K. Chan, *Spacecraft Collision Probability*, El Segundo, CA: Aerospace Press, 2008, pp. 77-82.

[26] European Space Agency, “DISCOSweb”, *Space Debris User Portal*. [Online]. Available: https://discosweb.esoc.esa.int. [Accessed: Aug. 12, 2024].

[27] U.S. Strategic Command, *Space-Track.org*. [Online]. Available: https://www.space-track.org. [Accessed: Jan. 29, 2024].